XLIII CILAMCE
21-25, November, 2022
FOZ DO IGUAÇU – PR – BRAZIL

Nonlinear transient vibrations of an orthotropic silo longitudinally stiffened considering the charging/discharging of the grains

Henrique de O. Pereira[1], Frederico M. A. da Silva[2]

Escola de Engenharia Civil e Ambiental; Universidade Federal de Goiás – UFG
Avenida Universitária, 1488, Qd. 86, Setor Leste Universitário, 74605-220, Goiás, Brasil
[1]henrique.pereira@discente.ufg.br, [2]silvafma@ufg.br

Abstract. The type of structure most used for the storage of grains are the cylindrical metallic silos, being slender structures in shell, which have great capacity to withstand the axial loads and the lateral pressures that are submitted. This paper aims to develop a low-dimensional model, with a reduced number of degrees of freedom, capable of analyzing the behavior of orthotropic and longitudinally stiffened silos subjected to static and dynamic axisymmetric actions. The nonlinear Sanders-Koiter theory is used to model the silo and Chebyshev polynomials are used to simulate the cantilever at the base and the free end in which these types of structures are commonly built. Grain pressures are determined according to the Janssen model, including the Heaviside function to simulate charging, and discharging inside the silo. In addition, the Heaviside function is also applied to the kinetic energy and the natural frequency of the system, to compose the variation of mass and damping generated by the grains over time. The motion equations are obtained by applying Hamilton's Principle and the Rayleigh-Ritz method and using the 4th order Runge-Kutta method, the maximum axial and transverse displacements during charging, and discharging are found, noting that an increase occurs when compared to the static values of grain storage, which generates greater efforts being applied to the silo structure.

Keywords: silos, nonlinear dynamic, low-dimensional model, grain pressure.

1 Introduction

The main objectives of grain storage are to maintain the quality of production, avoid large waste and provide regulation of the internal market. A substantial portion of grain storage is conducted in silos, with cylindrical metallic silos being the most used for this purpose. Structurally, cylindrical silos are defined as cylindrical shells, which have a great capacity to resist axial loads and lateral pressures, in addition to being relatively quick to build and easy to manufacture. To better understand the behavior of silos, Rotter and Sadowski [1] bring an analysis of the linear axisymmetric bending of orthotropic cylindrical shells, modeling the shell through Donnell's linear theory and investigating the stresses that arise in silo walls due to grain storage. Freitas [2] presents a theoretical and experimental study of grain pressures in flat-bottom cylindrical silos with a low height/diameter ratio, emphasizing the comparative analysis of the main theories and standards codes of grain pressures, considering that, for static pressures, the analytical theories of Janssen, Airy, Reimbert and Bischara. As most silos are built with stiffeners present in the structure, the stability of cylindrical metallic silos with corrugated walls and longitudinal stiffeners are studied by Iwicki et al. [3], determining the critical load of silos through nonlinear dynamic analysis and comparing the results obtained with the analytically predicted by the European standard code Eurocode 3.

Thus, the objective of the present work is to develop a low-dimensional dynamic model (few degrees of freedom) of an orthotropic cylindrical silo with externally fixed longitudinal stiffeners, capable of representing the charging and discharging behavior of the grains and the static pressures that these grains exert in the silo during the storage process, investigating, in a transient analysis, the variations of the maximum displacements and the maximum internal efforts that arise in the silo. In the mathematical formulation of the silo, the nonlinear Sanders-

Koiter theory is considered to describe the deformation field and changes in curvature of the mean surface of the slender silo and the orthotropic material considerations can describe the effects of the corrugate walls, leading a simple discrete model to evaluate the behavior of the silo in a pre-design scenario.

2 Mathematical formulation

It is considered a circular cylindrical shell of length *L*, average radius *R*, thickness *h* and with externally fixed longitudinal stiffeners that are separated from each other by a uniform distance d_s and with a center of gravity positioned at a distance e_s from the mid-surface of the shell. The axial, circumferential and radial coordinates of the shell are given, respectively, by *x*, θ and *z*, where the corresponding displacement fields are described by *u*, *v* and *w*, as illustrated in Figs. 1a,b.

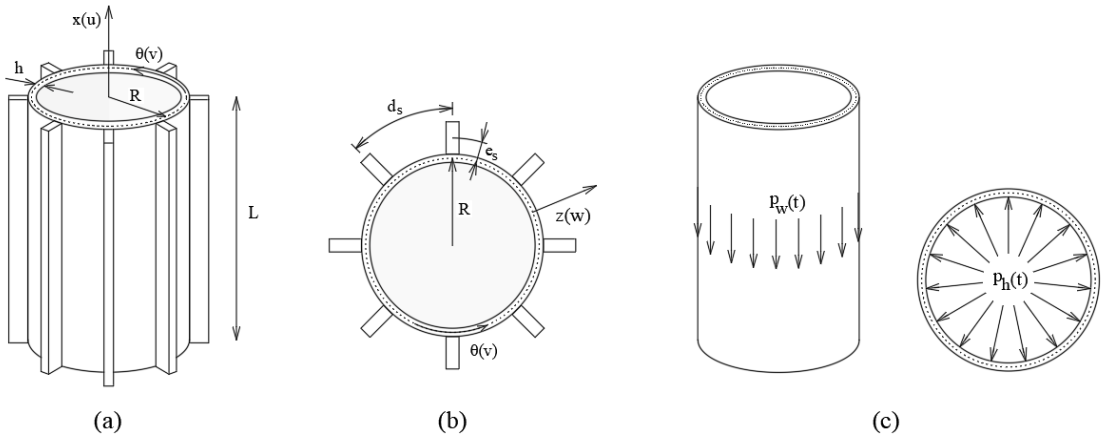

Figure 1. (a) Geometry and displacement fields of the shell, (b) distribution of stiffeners and (c) loading applied to the cylindrical shell.

The strain fields ε_x, ε_θ, and $\gamma_{x\theta}$ and the changes in curvature χ_x, χ_θ, and $\chi_{x\theta}$ of a point on the mid-surface of the shell are given, according to the Sanders-Koiter theory, by:

$$\varepsilon_x = u_{,x} + \frac{1}{2}w^2{}_{,x} + \frac{1}{8}\left(v_{,x} - \frac{u_{,\theta}}{R}\right)^2, \varepsilon_\theta = \frac{v_{,\theta}}{R} - \frac{w}{R} + \frac{1}{2}\left(\frac{w_{,\theta}}{R} + \frac{v}{R}\right)^2 + \frac{1}{8}\left(\frac{u_{,\theta}}{R} - v_{,x}\right)^2,$$
$$\gamma_{x\theta} = \frac{u_{,x}}{R} + v_{,x} + w_{,x}\frac{w_{,\theta}}{R} + w_{,x}\frac{v}{R},\ \chi_x = -w_{,xx}, \chi_\theta = \frac{-w_{,\theta\theta}}{R^2} - \frac{v_{,\theta}}{R^2}, \chi_{x\theta} = -\frac{w_{,x\theta}}{R} - \frac{3}{4}\frac{v_{,x}}{R} + \frac{1}{4}\frac{u_{,\theta}}{R^2}. \quad (1)$$

The relations between the stresses and deformations fields of the cylindrical shell, considering a plane stress state and a homogeneous, elastic, linear and orthotropic material, are defined according to the constitutive matrix:

$$\begin{Bmatrix} \overline{\sigma}_x \\ \overline{\sigma}_\theta \\ \overline{\tau}_{x\theta} \end{Bmatrix} = \begin{bmatrix} C_{11} & C_{12} & 0 \\ C_{21} & C_{22} & 0 \\ 0 & 0 & C_{33} \end{bmatrix} \begin{Bmatrix} \varepsilon_x + z\chi_x \\ \varepsilon_\theta + z\chi_\theta \\ \gamma_{x\theta} + 2z\chi_{x\theta} \end{Bmatrix}. \quad (2)$$

Where $\overline{\sigma}_x$, $\overline{\sigma}_\theta$, and $\overline{\sigma}_{x\theta}$ are, respectively, the normal stresses and the shear stress at any point in the shell C_{ij} (i, j = 1, ... ,3) are the coefficients of the elastic constitutive matrix of the orthotropic material given by:

$$C_{11} = \frac{E_x}{1 - \nu_{x\theta}\nu_{\theta x}}, C_{12} = \frac{\nu_{\theta x}E_\theta}{1 - \nu_{x\theta}\nu_{\theta x}}, C_{33} = G_{x\theta}, C_{22} = \frac{E_\theta}{1 - \nu_{x\theta}\nu_{\theta x}}, C_{21} = \frac{\nu_{x\theta}E_x}{1 - \nu_{x\theta}\nu_{\theta x}}. \quad (3)$$

Where E_x, E_θ, and $G_{x\theta}$ are the longitudinal, circumferential, and shear modulus of elasticity, respectively; and, $\upsilon_{x\theta}$ and $\upsilon_{\theta x}$ are the Poisson coefficients of the orthotropic shell. For orthotropic materials, it must be guaranteed that $C_{12} = C_{21}$, where the equality condition $\upsilon_{\theta x} E_x = \upsilon_{x\theta} E_\theta$ must be satisfied. It is important to highlight in this article

that the main orientation of the material coincides with the x and θ directions of the cylindrical shell in Figs. 1a,b. To determine the nonlinear equations of motion of the silo, a perfect cylindrical shell with grains is considered, generating an internal lateral pressure p_h and a tangential pressure to the surface of the shell p_w, which vary according to the height of stored grains, as shown in Fig. 1c. The internal pressures in the structure due to the stored grains are defined according to Janssen's theory [4], known as the elementary layer method. The static horizontal pressure p_h and the static frictional pressure p_w of the grains on the silo wall are given by:

$$p_h(x) = \frac{\rho_g}{\mu}\frac{A}{P_{er}}(1 - e^{-(L-x)K_s\mu A/P_{er}}), p_w = \mu p_h \,. \tag{4}$$

Where ρ_g is the density of the stored grain, μ is the coefficient of friction between the grain and the silo wall, A is the cross-sectional area of the silo, P_{er} is the perimeter of the silo cross-section, and K_s is the pressure ratio horizontal and vertical pressure of the silo.

In addition to the static storage loads, silos are also subject to the charging/discharging effects of the grains. To simulate these effects, this work considers the dynamic horizontal pressure of the grains as shown:

$$p_h(x,t) = \frac{\rho_g}{\mu}\frac{A}{P_{er}}[1 - e^{-(L_f-x)K_s\mu P_{er}/A}][H(x) - H(x - L_f)] \,. \tag{5}$$

Where $H(\ )$ is the Heaviside function and the term L_f varies with time for the charging process, eq. (6), or to simulate the discharge action, eq. (7).

$$L_f = L - \varepsilon t, \tag{6}$$

$$L_f = \varepsilon t. \tag{7}$$

Being t the time and ε the charging/discharging speed given in *m/s*. This velocity is established by making the relation with the mass flow of the grains, based on the analytical formulation of Hagen-Berveloo [5]:

$$\dot{m}_o = \rho_g g^{1/2} D_o^{5/2}. \tag{8}$$

Where $\dot{m}_o$ is the exit velocity of the grains, given in *kg/s*, g is the acceleration due to gravity and D_o is the diameter of the exit hole. In this way, the velocity ε is found by establishing the velocity in *m/s* equivalent to the loading or unloading in *kg/s* found in the Hagen-Beverloo equation.

Once the loads acting on the system are established, the nonlinear equations of motion are determined from the energy functionals of the system and, later, applying Hamilton's principle to the Lagrangian of the problem, which is defined as the difference between the energy kinetic T and the total potential energy Π. The kinetic energy T of the system is described by:

$$T = \frac{1}{2}\int_0^L\int_0^{2\pi} \rho_{eq} hR(\dot{u}^2 + \dot{v}^2 + \dot{w}^2)d\theta dx + \frac{1}{2}\int_0^L\int_0^{2\pi} RM\dot{w}^2[H(x) - H(x - Lf)]d\theta dx. \tag{9}$$

Where the first integral of the kinetic energy is related to the kinetic energy of the shell and the stiffeners, where $\dot{u}$, $\dot{v}$ and $\dot{w}$ are the axial, circumferential and radial velocities of the silo, respectively, and ρ_{eq} is the equivalent density of the structure that consider the total mass of cylindrical shell and stiffeners. The second integral of the kinetic energy is due to the grain mass M (mass per unit lateral area of the cylinder, given in *kg/m²*) which varies over time to account the loading/unloading effects of the grains according to the internal Heaviside function.

The total potential energy is defined as the difference between the internal deformation, eqs. (10) and (11), energy of the system and the work done by the external loads, eq. (12).

$$U_c = \frac{R}{2}\int_0^L\int_0^{2\pi}\int_{-h/2}^{h/2} (\overline{\sigma}_x\overline{\varepsilon}_x + \overline{\sigma}_\theta\overline{\varepsilon}_\theta + \overline{\tau}_{x\theta}\overline{\gamma}_{x\theta})dzd\theta dx. \tag{10}$$

$$U_e = \frac{1}{d_s}\int_0^L\int_0^{2\pi}[\frac{E_e}{2}(A_e\varepsilon_x^2 - 2e_sA_e\varepsilon_x w_{,xx}^2 + I_{0e}w_{,xx}^2) + \frac{G_eJ_e}{2}w_{,x\theta}^2]d\theta dx. \tag{11}$$

$$W_c = R\int_0^L\int_0^{2\pi}(p_h w - p_w u)d\theta dx. \tag{12}$$

Considering the system as a non-conservative system, eq. (13) describes the virtual work of viscous damping dissipative forces.

$$\delta W_{nc} = \int_0^L\int_0^{2\pi}[2\zeta\rho_{eq}h\omega_0(t)(\dot{u}\delta u + \dot{v}\delta v + \dot{w}\delta w)]Rd\theta dx. \tag{13}$$

Where ζ is the viscous damping coefficient and ω_0(t) is the lowest natural frequency of the shell in radians per second. In this work, the natural frequency of the system varies with time, since the total mass of the system (shell, stiffeners and grains) varies with time in the grain charging/discharging process.

It is observed that the free-fixed boundary condition is usually used in the design of the silo structural system, being clamped at the bottom (*x=0*) and free at the top (*x=L*). To satisfy the boundary conditions, consider the following modal expansions for the displacement fields *u*, *v* and *w*:

$$\begin{aligned} U(\eta,\theta,t) &= \sum_{m=0}^{M_U}\sum_{n=0}^{N}U_{m,n}(t)T_m^*(\eta)\cos(n\theta), \\ V(\eta,\theta,t) &= \sum_{m=0}^{M_V}\sum_{n=0}^{N}V_{m,n}(t)T_m^*(\eta)\cos(n\theta), \\ W(\eta,\theta,t) &= \sum_{m=0}^{M_W}\sum_{n=0}^{N}W_{m,n}(t)T_m^*(\eta)\cos(n\theta). \end{aligned} \tag{14}$$

Where $\eta=x/L$, $T_m^*(\eta) = T_m(2\eta\text{-}1)$, T_m is the nth order of the first kind Chebyshev polynomial [6] and $U_{m,n}(t)$, $V_{m,n}(t)$ and $W_{m,n}(t)$ are the modal amplitudes of the displacement fields *u*, *v* and *w*, respectively.

The equilibrium equations of the system are obtained by initially applying Hamilton's principle, given by:

$$\int_{t_1}^{t_2}\delta^1(T - (U_c + U_e - W_c))dt + \int_{t_1}^{t_2}\delta W_{nc}dt = 0. \tag{15}$$

And then, applying the fundamental lemma of variational calculus, the equilibrium equations are obtained, which can be represented by:

$$\frac{d}{dt}\frac{\partial\bar{L}}{\partial\dot{\mathbf{U}}} - \frac{\partial\bar{L}}{\partial\mathbf{U}} = \mathbf{R}. \tag{16}$$

Where **U** is the vector of displacement fields, $\dot{\mathbf{U}}$ the vector of velocity fields and **R** the vector of dissipative forces. So, substituting a chosen displacement, eq. (14), into eq. (16), a discretized system with $(M_u+M_v+M_w)$xN nonlinear second-order differential equations are obtained. It is important to notice that, due to the mass of grain to vary in time, this system of discretized differential equation has time-varying coefficients. The 4-th order Runge-Kutta method is used to obtain the system response over time.

3 Numerical Results

A cylindrical silo filled with soybeans is considered, with the bottom clamped and the top free, with a length L = 24 m, thickness of h = 0.01 m and radius R = 4 m. The longitudinal stiffeners are equally spaced in 0.62 m and they have a square cross section with 0.05 m. Soybean grains have density ρg = 800 kg/m³, lateral pressure coefficient Ks = 0.63 and friction coefficient with the silo wall μ = 0.38 [7].

To validate the analytical model proposed for the structure of the silo, Table 1 presents the maximum transverse displacement, normalized by the shell thickness, obtained in the present work for different modal expansions of the displacement field (12 DOF – M_U=M_V=M_W=4, N=0; e, 15 DOF – M_U=M_V=M_W=5, N=0) and different considerations of the orthotropic material. Then, the obtained results are compared with those obtained from the finite element method, using the commercial software Abaqus with a previously tested finite element mesh that guarantees the convergence of the results provided by the software. Setting the Poisson ratio at $\upsilon_{x\theta}$=$\upsilon_{\theta x}$=0.30 and the longitudinal modulus of elasticity at E_x =200 GPa, and, varying the modulus of elasticity in E_θ, the low-dimensional model results present with a difference, relative to the Abaqus results, less than 8%, when a solution with 12 DOF was used, and less than 6% when a modal expansion with 15 DOF was used. The results presented in Table 1 were considered satisfactory for the developed low-dimensional model.

Table 1. Maximum normalized transverse displacements of the silo, with orthotropic properties, filled with soybeans.

E_x/E_θ	Maximum transverse displacement			Difference (%)	
	Present work – 12 DOF	Present work – 15 DOF	Abaqus	Present work – 12 DOF	Present work – 15 DOF
2,00	0,141	0,144	0,152	7,65	5,93
1,50	0,108	0,110	0,115	6,74	4,96
1,25	0,091	0,093	0,096	5,18	3,36
0,80	0,062	0,063	0,063	1,13	0,87
0,67	0,053	0,055	0,053	0,58	2,69
0,50	0,043	0,044	0,042	1,93	4,29

Then, using the same geometry of the silo described and using the model with 12 GDF, a transient analysis of the axial and transverse displacements and the efforts was conducted, for the complete charge and discharge of the silo, for two orthotropy relations. The values of the displacements found were normalized in relation to the thickness of the shell and the results over time were obtained at a point where the values are maximum, being for L = 24 m in the axial displacements and L = 6 m in the transverse displacements.

Initially, for discharging of the silo, it was considered the exit hole diameter of 1/4 of the silo diameter, which represents a complete discharging in 96 seconds (represented by the vertical dashed line in Figs. 2-5). From the results indicated in Fig. 2(a,b), an increase in the axial and transverse displacements can be seen in relation to the values found for the static storage (represented by the horizontal dotted lines), right at the beginning of the discharge. For the axial displacements (Fig. 2(a)), the two cases of orthotropy present similar values and behavior, presenting high vibrations when the discharging starts. For transversal displacements (Fig. 2(b)), the orthotropy ratio has a greater effect on the results, leading the displacements up to three times higher at the beginning of discharging for the ratio E_x/E_θ = 2. In Figs. 3 (a,b), the internal membrane N_x $(= \int \bar{\sigma}_x dz)$ and bending M_x $(= \int \bar{\sigma}_x z dz)$ resultants over time at the bottom of the silo, normalized with the values obtained in the static storage, are obtained. For these two internal resultants, it is observed that the orthotropy does not have a representative influence at the beginning of the discharging process, amplifying N_x and M_x internal resultants in 40% and 60%, respectively, when compared with the static values.

When the silo is charging, it was considered a total time of 96 seconds for complete filling. From the results indicated in Figs. 4 (a,b), a large vibration can be seen in the initial time for the axial (Fig. 4(a)) and transversal (Fig. 4(b)) displacements. It is important to notice that the silo presents a variation between axial elongation and shortening, as shown in Fig. 4 (a). In Figs. 5 (a,b), it can be seen that an envelope of forces resulting from the vibration of the silo, in which traction and compression of the N_x and inversion of the M_x occur in the initial time, until they stabilize in the statics results. This behavior was not observed in the discharging process.

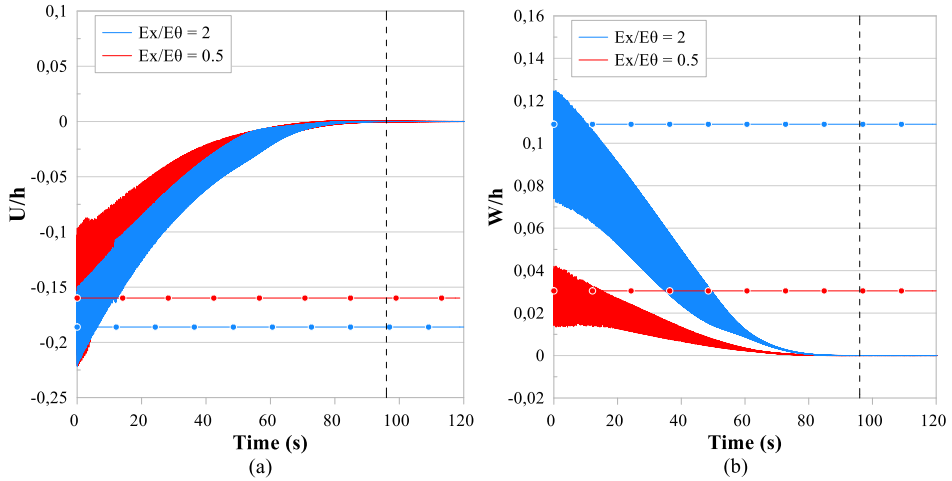

Figure 2. Time response of (a) axial and (b) transversal displacements considering the discharging of the silo.

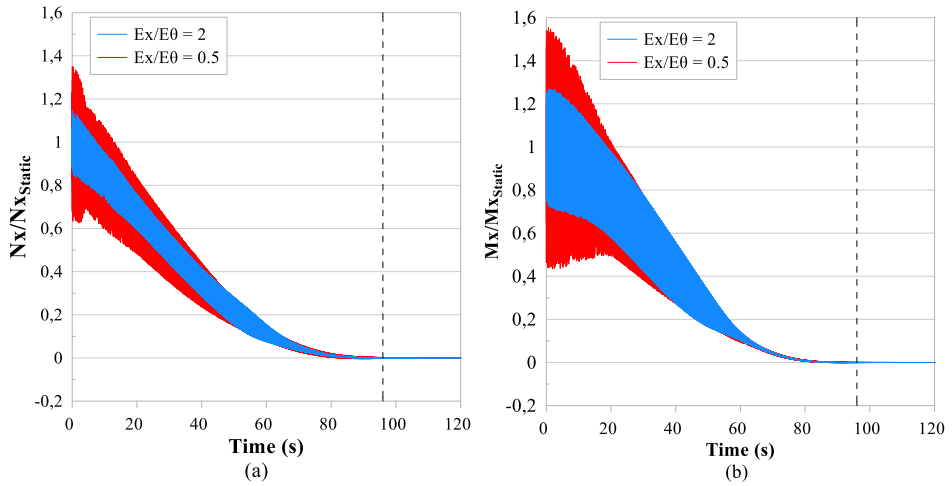

Figure 3. Time response of axial (a) membrane and (b) bending internal resultants considering the discharging of the silo.

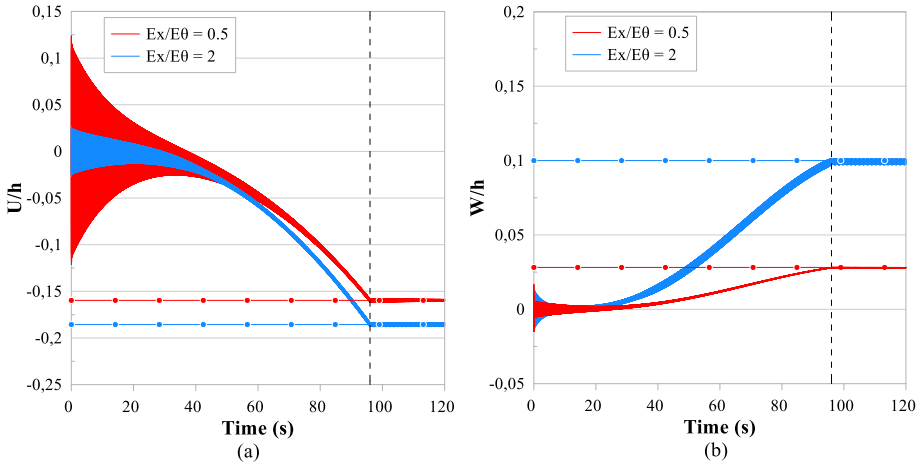

Figure 4. Time response of (a) axial and (b) transversal displacements considering the charging of the silo.

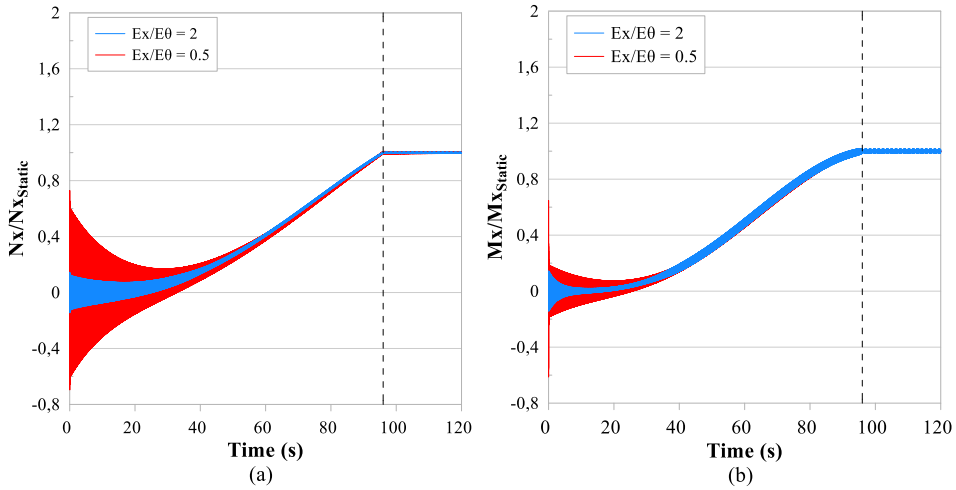

Figure 5. Time response of axial (a) membrane and (b) bending internal resultants considering the charging of the silo.

4 Conclusions

The nonlinear Sanders-Koiter theory is used to develop a low-dimensional model of an orthotropic and longitudinally stiffened silo. The nonlinear equations of motion are obtained from the Lagrangian of the system, in which the Chebyshev polynomials were used to satisfy the clamped-free boundary conditions of the silo. The consideration of the charging/discharging of the soybeans were inserted in the kinetic energy and in the load's work to represent their variation along the time. A numerical validation was conducted comparing the obtained results with a model developed from the finite element method, in which it was found that the model with 12 DOF are satisfactory to represent the behavior of the silo. From this, a transient analysis, obtained by the 4-th order Runge-Kutta method, of the axial and transversal displacements and internal membrane and bending in the axial direction during charging/discharging of the silo, was conducted, in which it was observed that there is an amplification of these effects. The low-dimensional model derived for a stiffened orthotropic cylindrical silo can analyze the nonlinear behavior under static and dynamic axisymmetric actions in a pre-design scenario.

Authorship statement. The authors hereby confirm that they are the sole liable persons responsible for the authorship of this work, and that all material that has been herein included as part of the present paper is either the property (and authorship) of the authors, or has the permission of the owners to be included here.

References

[1] J.M. Rotter and J.A. Sadowski, "Cyllindrical shell bending theory for orthotropic shells under general axisummetric pressure distibutions". *Engineering Structures*, pp. 258-265, 2012.
[2] E.G.A. Freitas. Estudo Téorico e experimental das pressões em silos cilíndricos de baixa relação altura/diâmetro e fundo plano. PhD Thesis, University of São Paulo, 2001.
[3] P. Iwicki, K. Rejowski and J. Tejchman, "Stability of cylindrical steel silos composed of corrugated sheets and columns based on FE analyses versus Eurocode 3 approach". *Engineering Failure Analysis*, pp. 444-469, 2015.
[4] F. Ayuga, "Los empujes del material almacenado em silos". *Informes de la Construcción*, vol. 46, 1995.
[5] M. Pliego, C.A. Vargas and A. Medina, "On the validity of the Hagen and Berveloo formulas for grains discharge through thin shidewalls of bins". *Mexican Journal of Physics*, pp. 139-147, 2019.
[6] M. Amabili and Y. Kurylov. "Polynomial versus trigonometrix expansions for nonlinear vibrations of circular cylindrical shells with different boundary conditions". *Journal of Sound and Vibration*, vol. 329, pp. 1435-1449, 2012.
[7] Eurocode 1: Actions on structures – Part 4: Silos and tanks. The European Union, 2006.